University of Huddersfield

University of Huddersfield Repository

Kollar, László E., Farzaneh, Masoud and Van Dyke, Pierre

Modeling Ice Shedding Propagation on Transmission Lines with or without Interphase Spacers

Original Citation

Kollar, László E., Farzaneh, Masoud and Van Dyke, Pierre (2013) Modeling Ice Shedding Propagation on Transmission Lines with or without Interphase Spacers. IEEE Transactions on Power Delivery, 28 (1). pp. 261-267. ISSN 0885-8977

This version is available at http://eprints.hud.ac.uk/16066/

http://eprints.hud.ac.uk/

Modeling Ice Shedding Propagation on Transmission Lines with or without Interphase Spacers

László E. Kollár, Masoud Farzaneh, *Fellow IEEE,* and Pierre Van Dyke

Abstract—Ice shedding propagation on a single conductor and on a circuit of three conductors in a vertical configuration where conductors are linked with interphase spacers was modeled numerically. Several concentrated loads acting along the loaded span modeled the ice, and the shedding propagation was then simulated through the removal in a defined sequence of these concentrated loads. The model determines conductor displacement and the variation of conductor tension during the vibration following ice shedding propagation; and thus, it predicts conductor rebound height, tension peak, and to what extent the conductor clearance is reduced during vibration. Ice shedding propagation on the full-scale test line of Hydro-Quebec was considered, and the model was validated by comparing simulation results to former experimental observations. Results show that the application of spacers reduces the severity of vibration considerably, and consequently increases the conductor clearance and reduces the risk of flashover. The dynamic effects of different shedding processes were also compared. The rebound height is the greatest for a single conductor when ice detachment propagates along the conductor, but then ice falls suddenly as a big chunk. However, the consequences of sudden detachment and shedding are obtained the most severe when conductors are linked with spacers.

Index Terms—Conductors, Ice, Simulation, Transmission line modeling, Vibrations

L. E. Kollár and M. Farzaneh are respectively member and chairholder of the NSERC/Hydro-Quebec/UQAC Industrial Chair on Atmospheric Icing of Power Network Equipment (CIGELE) and Canada Research Chair on Atmospheric Icing Engineering of Power Networks (INGIVRE), http://www.cigele.ca, University of Quebec at Chicoutimi, 555 boulevard de l'Université, Chicoutimi, QC, Canada, G7H 2B1 (corresponding author: L. E. Kollár; phone: 418-545-5011/5606; fax: 418-545-5012; e-mail: laszlo_kollar@uqac.ca and farzaneh@uqac.ca).

P. V. Dyke is with Hydro-Quebec Research Institute (IREQ), 1800 boul. Lionel-Boulet, Varennes, QC, Canada, J3X 1S1 (e-mail: vandyke.pierre@ireq.ca).

I. INTRODUCTION

ICE shedding from transmission line conductors may cause serious dynamic effects on the power line elements depending on the ice shedding process. Ice may shed in small pieces and the shedding propagates along the span or part of the span with its associated sudden release of the additional weight of the ice. In other cases, the ice detachment propagates along the span, but the detached ice chunk does not fall immediately because it remains connected to other parts of the ice accretion, and when it finally falls, it exerts an additional pull on the conductor due to its downward gravity acceleration. A third possibility is the sudden ice shedding from the entire span or from a long part of it, when a big ice chunk is detached from the conductor and falls suddenly.

Ice shedding, and consequently unloading a significant part of the conductor, leads to conductor jump and vibration and excessive transient dynamic forces. High conductor rebound may trigger flashovers whereas the dynamic loads may cause suspension failure and even cascading damage to several towers. Spacer dampers in conductor bundles may help to attenuate cable vibration, whereas interphase spacers may contribute avoiding the contact between phases. However, their application increases the load on the conductors and on the related structure. When a shedding conductor is linked to other conductors by spacer dampers or by interphase spacers, the rotation of the spacer or the bundle may also be significant, leading to bundle collapse in extreme cases. A review of ice-related dynamic problems on overhead lines, including ice shedding and bundle rolling is provided in [1]. These problems justify the particular interest in cold climate regions to predict the conductor jump height and transverse movement as well as the tension developing in the conductor and at the suspension during vibration following ice shedding.

Field observation of ice shedding is a difficult task, because of the unforeseeable and non-repetitive occurrence of the phenomenon. Therefore, great effort has been made to simulate ice shedding numerically and experimentally on small-scale or full-scale test lines in order to understand the dynamic effects of ice shedding. Numerical models have been developed to simulate ice shedding from a single conductor [2], [3] or from conductor bundles [4], [5]. Experiments were carried out on small-scale experimental setup [2] as well as

full-scale test line [6]. All of these models and tests considered sudden ice shedding, whereas propagating ice shedding was simulated on a full-scale test line in [7], in small-scale experiments in [8], and numerically on a single conductor in [9].

The numerical model of [9] is improved in the present study so that it would be applicable to simulate ice shedding propagation on several spans of conductors linked with interphase spacers, and the model is validated by comparing simulation results to experimental observations on a full-scale test line [7]. The model is applied to predict vertical and transverse conductor displacement and conductor tension variation during the vibration initiated by ice shedding propagation. A further goal involves the comparison of the dynamic effects of the three shedding processes mentioned above, i.e. (i) propagation of ice shedding along the length of the span, (ii) propagation of ice shedding along the length of the span plus an additional downward pull induced at discrete locations along the span by the detachment of ice chunks, and (iii) sudden and simultaneous ice shedding from the whole span or part of the span.

II. NUMERICAL MODELING

This section describes the numerical model of the transmission line elements (cable, suspension strings, and spacers), as well as the ice load, and the different processes of ice shedding. The model is implemented using the finite element analysis software ADINA [10].

A. Cable, Suspension Strings, and Spacers

The model of the cable and the suspension strings is based on former recommendations [2], [3]. The cable is modeled by two-node isoparametric truss elements with large kinematics. A constant initial pre-strain corresponding to the installation conditions is prescribed as an initial condition for all cable elements. This initial strain may be obtained from the horizontal tension in static equilibrium of the catenary and the cable geometrical and material properties [11]. The material properties of the cable are accounted for by a nonlinear elastic material model, not allowing compression and assuming Hookean small-strain behaviour in tension. The cable is assumed to be perfectly flexible in bending and torsion. The cable damping is considered as Rayleigh damping as proposed in [12]. The Rayleigh damping coefficients are obtained from the natural circular frequencies and the corresponding damping ratios in two different vibration modes of the cable. The suspension strings are modelled with beam elements using isotropic linear elastic material properties with constant cross-section. Interphase spacers are considered as simple rods clamped to a conductor at each end. They are modeled with beam elements, and are associated with an isotropic linear elastic material.

B. Ice Load and Ice Shedding Processes

Ice load is modeled by several concentrated loads acting at constant distances along the loaded span. Although ice usually appears on conductors as a distributed load, concentrated loads can be applied on truss elements unlike distributed loads, and the application of concentrated loads simulates more adequately the ice load of the experimental ice shedding tests where the loads were also attached at several discrete points along the span. If these concentrated loads are attached to enough points of the cable, they provide a satisfactory approximation of the distributed ice load and its static and dynamic consequences as was shown in [5]. Ice shedding propagation is then simulated through the removal in a defined sequence of the concentrated loads. The propagation velocity is controlled by associating each concentrated load with a time function which determines the removal time of that specific load. In the calculation, the load is multiplied in each time instant by the value the time function takes in that time instant. The three ice shedding processes mentioned in Section I may be modeled by using two different time functions which were proposed in [9]. In both time functions, the time, t_i, denotes the beginning of load removal, Δt_r stands for time interval of load removal, and Δt_s is the time step in the numerical simulation. It is assumed that a load is removed suddenly, i.e. $\Delta t_r < \Delta t_s$.

When ice shedding propagates along the span with its associated load removal, the time function shown in Fig. 1(a) is applied for each load at different time instances. If n loads act along the span and T_w denotes the wave propagation time along the span, then the time instance when the defined time function is applied for the ith load may be determined as follows:

$$t_i = \frac{i}{n+1} T_w \qquad i = 1,\ldots,n \qquad (1)$$

When ice detachment propagates along the span, but the ice falls in big chunks, then the detached ice does not break off the ice which is still attached to the remaining part of the conductor and applies an excess load on the conductor where the ice is still attached. Thus, a time function which considers a significant increase in the load locally before load removal should be applied as shown in Fig. 1(b). The time instance, t_i, when the time function is applied for the ith load is obtained from Eq. (1).

When ice is detached and falls suddenly in big chunks, then the time function presented in Fig. 1(a) is applied; however, the time instance of application, t_i, is the same for each load (i.e. for each $i = 1,\ldots,n$), which is the beginning of the dynamic analysis. This paper discusses the dynamic effects of the three shedding processes presented, but the numerical method may easily be adjusted to simulate further shedding processes: e.g. non-uniform ice load along the span may be modeled by

varying the magnitudes of the *n* loads; partial ice shedding may be simulated by applying time function only for some of the loads; and a non-constant propagating velocity can also be considered by modifying Eq. (1), i.e. the time instance of application of time function.

C. Procedure of Computation

The initial profile, i.e. the profile of the unloaded span is determined using the catenary equation [11]. The initial configuration was then constructed in ADINA, and the point loads simulating the accumulated ice were added in the static analysis that provided the loaded profile of the modeled configuration. The time function describing the shedding propagation is defined and applied in a separate, dynamic analysis that simulates the load removal and the resulting cable vibration in the following few seconds. The related governing equations solved numerically in ADINA are presented in [13], and a detailed description of the applied finite element procedures is provided in [14].

III. SIMULATION OF ICE SHEDDING PROPAGATION ON HYDRO-QUEBEC FULL-SCALE TEST LINE

A. Construction of Numerical Model

The Hydro-Quebec test line consists of three suspension spans and two dead-end spans. Ice shedding propagation on the middle span from a single conductor and from a conductor in a vertical arrangement of three conductors was simulated in [7]. Two of these tests (called Test A and Test C in [7]) are modeled numerically in the present paper. Figs. 2(a) and 2(b) sketch the numerical model of the unloaded test line with single conductors (Test A), and that of the middle span with the vertical arrangement of three conductors (Test C), respectively. In the latter case, the top and bottom conductors are in the same vertical plane, but there is a transverse distance of 0.98 m between the vertical plane of the middle conductor and that of the other two conductors. Each suspension span includes 150 cable elements, whereas the dead-end spans consists of 50 cable elements. The ice shedding tests were performed on Condor ACSR 54/7 conductors suspended with glass I-insulator strings. The conductor damping is due mainly to aerodynamic resistance whereas structural damping was found several orders of magnitude smaller [15]. The damping coefficient due to aerodynamic resistance was determined in several tests in [15], and values around 0.01 were obtained in the first vibration mode. The Rayleigh damping coefficients were calculated using this damping ratio and the natural circular frequencies in the first symmetric and antisymmetric modes. In the tests with three conductors per span, the conductors in each span were linked with four interphase spacers located at one third and one fourth of the span length as shown in Fig. 2(b). Details of these interphase spacers are provided in [15]. The numerical model considers these spacers with constant cross section and with material properties defined for aluminum for simplicity.

Ice weight was modeled in the experiments of [7] by a conductor which was held initially by pulleys at each end of the span, and which was connected to the test conductor by strings at every 15 m along the span. Shedding was initiated by releasing the pulley at the end of the span near Tower 2, and then the strings broke one after the other simulating the propagation of load shedding toward Tower 3. Similarly, the numerical model simulated shedding starting from Tower 2 and propagating toward Tower 3. Correspondingly, concentrated loads were considered at every 15 m, thereby applying *n* = 29 loads along the 450-m-long middle span. Since the shedding process in the experiments was closest to the propagation of ice detachment followed by falling of a big chunk, the time function shown in Fig. 1(b) was applied in the numerical model with time instance of application, t_i, defined by Eq. (1). In Test A, a load of 0.6 kg/m was applied on the conductor in the middle span, and it took 3 s to break all the strings holding the dead-weight conductor (i.e. $T_{w,A}$ = 3 s). This load corresponds to the weight of 6-mm-thick cylindrical ice accretion on Condor conductor if glaze ice with density of 900 kg/m^3 is assumed. In Test C, the three conductors in the middle span were loaded initially. The load on the top and mid conductor was 2.37 kg/m (corresponding to ice thickness of 18 mm), whereas the load on the bottom conductor was 1.5 kg/m (corresponding to ice thickness of 13 mm). Since the top and mid conductors remained loaded during the test, they were loaded in the experiments by attaching D-shapes to them with additional masses. Consequently, the cross section of these two conductors was increased in the numerical model in order to consider the load on them. The bottom conductor was unloaded during the test, and the whole span was unloaded in 16 s (i.e. $T_{w,C}$ = 16 s).

B. Simulation Results

This section compares results of numerical simulations and experimental observations reported in [7] and in [15] for Tests A and C. The load is applied in the static analysis, when the displacement and tension in the loaded conductor are determined. Then, the dynamic analysis calculates the conductor rebound height together with the time histories of conductor displacement and tension.

The results of static analysis are shown in Table 1. For Test A, there is an excellent agreement between the calculated and measured additional displacements at mid-span. However, the additional displacement was measured as 3.00 m at 150 m from Tower 3, whereas the maximum displacement was calculated numerically at mid-span (i.e. 225 m from Tower 3). Thus, the calculated displacements at positions on the side of Tower 3 are smaller than the measured ones. For Test C, the discrepancy between the calculated and measured additional displacements at mid-span is still small, below 10%; but similarly to Test A, the asymmetry of the profile was more significant in the measurements. The maximum displacement was measured as 2.52 m at 150 m from Tower 3, whereas the

displacements on the side of Tower 2 were measured smaller than those in the calculated loaded profile. There is an asymmetry in the entire configuration due to the different lengths of the neighboring spans and to the asymmetric positions of the interphase spacers along the span in Test C; however, further factors may cause additional asymmetry, which were not considered in the model. The cable tension in the loaded span was calculated within 2-3% of the measured value for both of Tests A and C.

Results of dynamic analysis are compared to experimental observations in Figs. 3, 4 and 5 and in Table 2. The maximum vertical displacements of the conductor above the loaded position at different distances from the suspension are shown in Fig. 3. The model provides a close approximation of experimental results for Test A. Model predictions for Test C are within 10% compared to the experiments at 75 m from Tower 3 and at mid-span (225 m), but a considerable discrepancy occurs at 150 m, 300 m and 375 m. These discrepancies are mainly the consequences of those that were already in the profile after applying the load. The displacements in the numerical static analysis were smaller on the side of Tower 3 and greater on the side of Tower 2 than in the experiments, and the same tendency holds for the conductor jump after shedding. Both of the experimental and numerical results suggest that the maximum conductor rebound above the loaded position is reduced by half (from about 6 m to about 3 m) when using interphase spacers. Since the vertical distance between phases in static equilibrium was 3.65 m (see Fig. 2(b)), the risk that conductors touch each other during vibration is reduced significantly by the application of interphase spacers.

Figure 4 compares the time histories of conductor displacement when shedding propagates along the span from 0 to 3 s in Test A and from 0 to 16 s in Test C. These time histories show clearly that the conductor drops at the position where the shedding takes place, and then it jumps. In Test A, shedding propagates along the 450-m-long span in 3 s; thus, it arrives to 375 m, 225 m, and 75 m from Tower 3 after 0.5 s, 1.5 s, and 2.5 s, respectively. The conductor at these points reaches its lowest position in these time instances, and then it moves upward quickly. The maximum rebound of the single conductor according to the numerical simulation appears at 190 m from Tower 3, i.e. it is farther from the tower where the shedding propagation begins and closer to the tower which is connected to the longer span. In Test C, the shedding propagation arrives to mid-span after about 8 s, when the conductor reaches its lowest position. The maximum rebound appears at about 250 m from Tower 3, which is close to the half distance between the two interphase spacers located at 150 m and 336 m from Tower 3.

Some data related to the displacement time histories, namely the conductor drop before shedding, the maximum conductor rebound after shedding, and the period of vibration, are listed in Table 2 for Test A. The calculated and measured conductor drops at 375 m from Tower 3 coincide, but then the model predicts increasing drop along the span, whereas it was measured greater at mid-span than at 75 m from Tower 3. Contrarily, the model overestimates the first peak at 375 m, whereas the prediction is excellent (2-3% discrepancy compared to measured results) at mid-span and at 75 m. The period of vibration coincides; it is about 6 s in both of the experiments and the numerical simulations. Concerning Test C, the model provides an excellent estimation of the conductor drop at mid-span, it underestimates the peak by about 10%, and this peak appears about 4 s earlier than in the experiments (see Fig. 4(d)).

The time histories of conductor tension at mid-span are presented in Fig. 5. The tension increases approximately at the same time when the conductor drops, and then decreases to the value which was observed without the load. The model provides an excellent prediction for Test A, and the tendency obtained numerically also follows the measured one for Test C, but in this case the model does not predict the increase in the tension before load shedding.

IV. SUDDEN AND PROPAGATING SHEDDING ON CONDUCTORS LINKED WITH SPACERS

When ice detachment propagates along the span and ice falls in small pieces, then the conductor rebound also propagates along the span. When the propagation of ice detachment is followed by falling of a big chunk, then the conductor rebound propagates, but a drop precedes the upward movement, and the rebound height is higher due to the increasing load before load removal. This process was discussed in detail in Section III.B. When the ice is detached from the conductor suddenly, then the whole conductor jumps immediately. For the sake of simplicity, these processes will be referred to as propagating shedding, propagating detachment followed by sudden fall, and sudden shedding, respectively. The numerical model is applied to simulate these three shedding processes on the Hydro-Quebec test line in the same configurations as in Tests A and C. Thus, the static analysis and the resulting loaded profile are the same in the different shedding processes, but the dynamic analysis considers various load removal processes by applying different time functions as discussed in Section II.B. Shedding from the entire span is considered in these simulations.

The maximum vertical displacements of the conductor above the loaded position at different distances from the suspension are compared in Fig. 6. For a single conductor, there is no significant difference in the conductor rebound heights after propagating shedding and sudden shedding, but they are 10-30% greater after propagating detachment followed by sudden fall. This can be explained by the load increase before removal. It can also be observed that the maximum conductor rebound appears at mid-span after sudden shedding, but in the other two cases it is farther from the tower where the shedding propagation begins. For the three-conductor configuration, the conductor rebound heights after

propagating detachment followed by sudden fall are about 10-30% greater than after propagating shedding, and they are an additional 10-30% greater after sudden shedding. Thus, the application of interphase spacers reduces conductor movement to a greater extent after propagating shedding or after propagating detachment followed by sudden fall than after sudden shedding. It should also be noted that the jump height is reduced at 150 m for the three shedding processes as may be observed in Fig. 6, which is due to the interphase spacer located exactly at this position.

Time histories of conductor vertical displacement at mid-span are also compared for the three shedding processes (Fig. 7). After sudden shedding, the conductor jumps upward immediately. In the other two cases, it vibrates with small amplitude at the beginning, but the jump is delayed until the propagation of ice detachment approaches mid-span. Since the propagation speed is greater in the configuration with single conductor than with three conductors, the delay is shorter in that case. When the detachment propagates followed by sudden fall, then the jump is preceded by a drop as was already discussed in Section III.B. Fig. 7(a) also shows that, although the rebound height is not the greatest after sudden shedding from a single conductor, the decay of vibration is slower in this case. In case of the three-conductor configuration, the rebound height is greatest and the decay of vibration is slower after sudden shedding (see Fig. 7(b)).

The relative motion of conductors in the configuration when conductors are linked with interphase spacers is also important, because it gives information whether the conductors touch each other during the vibration. The time histories of distance between the middle and bottom conductors at mid-span are shown in Fig. 8. Originally, the vertical and transverse distances were 3.65 m and 0.98 m, respectively. When the load is added, the transverse distance reduces, but the vertical distance increases, especially at locations far from the spacers. The total distance at mid-span becomes 4.17 m, which is the initial distance in Fig. 8. The conductors approach each other to the greatest extent after sudden shedding; however, the minimum distance is still 1.67 m. Thus, the interphase spacers can sufficiently reduce the severity of vibration in the case considered.

V. CONCLUSIONS

A numerical model has been developed to simulate different ice shedding processes on transmission lines with conductors linked with interphase spacers. The model was validated by applying to experimental ice shedding tests carried out on the Hydro-Quebec test line, and then it was used to compare the dynamic effects of three different shedding processes: (i) propagation of ice shedding along the span, (ii) propagation of ice shedding along the span with an additional downward pull on the conductor at the discrete locations where the ice chunks finally part from the conductor, and (iii) sudden and simultaneous ice shedding from the span or part of the span.

The model considered ice load by several concentrated loads applied along the span, which were then removed consecutively or suddenly depending on the simulated ice shedding process. The load removal was controlled by a time function which was adjusted according to the modeled phenomenon.

The model estimates the conductor profile and tension after the application of the load, and the time histories of conductor displacement and conductor tension during the vibration following shedding. These time histories also provide the conductor rebound height, the peak tension, and the minimum distance between conductors occuring during vibration. Simulation results show, in agreement with former experimental observations, that the application of interphase spacers may reduce conductor rebound height above the loaded position by a factor of two approximately, and thereby they contribute to prevent the reduction of conductor clearance during high-amplitude vibrations. The comparison of different shedding phenomena reveals that sudden shedding has the most severe dynamic effects for conductors linked with interphase spacers; however, the rebound height of a single conductor may be higher in the case of ice shedding with ice chunks pulling on the conductor before parting from the conductor.

REFERENCES

[1] D. G. Havard, P. Van Dyke, "Effects of Ice on the Dynamics of Overhead Lines. Part II: Field Data on Conductor Galloping, Ice Shedding and Bundle Rolling," in *Proc. of 11th International Workshop on Atmospheric Icing of Structures*, Montreal, QC, 2005, pp. 291-296.

[2] A. Jamaleddine, G. McClure, J. Rousselet, R. Beauchemin, "Simulation of Ice Shedding on Electrical Transmission Lines Using ADINA," *Computers & Structures,* vol. 47(4/5), pp. 523-536, 1993.

[3] M. Roshan Fekr, G. McClure, "Numerical modelling of the dynamic response of ice shedding on electrical transmission lines," *Atmospheric Research,* vol. 46, pp. 1-11, 1998.

[4] L. E. Kollár, M. Farzaneh, "Vibration of Bundled Conductors Following Ice Shedding," *IEEE Trans. on Power Delivery,* vol. 23(2), pp. 1097-1104, 2008.

[5] L. E. Kollár, M. Farzaneh, "Modeling Sudden Ice Shedding from Conductor Bundles," *IEEE Trans. on Power Delivery*, submitted for publication.

[6] V. T. Morgan, D. A. Swift, "Jump height of overhead-line conductors after the sudden release of ice loads," *Proc. of IEE,* vol. 111(10), pp. 1736-1746, 1964.

[7] P. Van Dyke, A. Laneville, "Simulated Ice Shedding on a Full-Scale Test Line," *Proc. of 8th Int. Symp. on Cable Dynamics,* Paris, France, 2009.

[8] L. E. Kollár, M. Farzaneh, "Numerical Modeling and Small-Scale Experimental Simulation of Ice Shedding Propagation on Bundled Conductors," *Proc. of 14th International Workshop on Atmospheric Icing of Structures,* Chongqing, China, 2011, Paper B6_3_ID225.

[9] L. E. Kollár, M. Farzaneh, P. Van Dyke, "Modeling of Cable Vibration Following Ice Shedding Propagation," *Proc. of 14th International Workshop on Atmospheric Icing of Structures,* Chongqing, China, 2011, Paper B5_3_ID224.

[10] ADINA, *Theory and Modeling Guide,* Watertown, MA, 2010.

[11] H. M. Irvine, *Cable Structures,* MIT Press: Cambridge, MA, 1981.

[12] M. Roberge, "A Study of Wet Snow Shedding from an Overhead Cable," M.Eng. thesis, Dept. Civil Eng. and Applied Mech., McGill Univ., Montreal, QC, 2006.

[13] L. E. Kollár, M. Farzaneh, "Dynamic Behavior of Cable Systems with Spacers Following Ice Shedding," *Proc. of ICNPAA 2006: 6th International Conference on Mathematical Problems in Engineering and Aerospace Sciences,* Paper 42, pp. 399-406, Budapest, Hungary, 2006.

[14] K.-J. Bathe, *Finite Element Procedures*, Prentice Hall, Upper Saddle River, New Jersey, 1996.

[15] P. Van Dyke, "Galop induit sur une ligne expérimentale à l'aide de profilés en D sur conducteur simple avec ou sans entretoises interphases," Ph.D. thesis IV-1793, Dept. Mech. Eng., Univ. of Sherbrooke, Sherbrooke, QC, 2007.

László E. Kollár received a M.Sc. degree in Mechanical Engineering from the Budapest University of Technology and Economics, Hungary in 1997, a Ph.D. degree in Mechanical Engineering from the same university in 2001, and a M.Sc. degree in Mathematics from the University of Texas at Dallas, USA in 2002.

In 2002, he joined CIGELE NSERC/Hydro-Quebec/UQAC Industrial Chair and INGIVRE Canada Research Chair at the University of Quebec at Chicoutimi as a Postdoctoral Fellow, where he currently is a Research Professor on grant. His research interests include theoretical and experimental modeling of atmospheric icing processes and ice shedding from cables. He previously worked on the modeling of controlled unstable mechanical systems with time delay. He authored or co-authored more than 40 journal and conference papers and a book chapter.

Masoud Farzaneh (M'83-SM'91-F'07) is Director-founder of the International Research Center CENGIVRE, Chairholder of the CIGELE NSERC/Hydro-Quebec/UQAC Industrial Chair and of the INGIVRE Canada Research Chair related to power transmission engineering in cold climate regions. He authored or co-authored about 500 technical papers, and 18 books or book chapters. Prof. Farzaneh has so far trained more than 100 postgraduate students and postdoctoral fellows. Actively involved with CIGRÉ and IEEE, he is Convenor of CIGRE WG B2.44 on coatings for protection of overhead lines during winter conditions, and member of the Executive Committee of CIGRE Canada. He is currently Administrative Vice-President of IEEE DEIS, and member of the Editorial Board of IEEE Transactions on Dielectrics and Electrical Insulation. He is Fellow of IEEE, Fellow of The Institution of Engineering and Technology (IET) and Fellow of the Engineering Institute of Canada (EIC). His contributions and achievements in research and teaching have been recognized by the attribution of a number of prestigious prizes and awards at national and international levels.

Pierre Van Dyke received a B.Eng. and M.Sc.A. degree from École Polytechnique de Montréal in 1983 and 1985 respectively, a Masters Certificate in Project Management from Laval University in 2005, and a Ph.D. degree from University of Sherbrooke, Canada in 2007.

He is currently Senior Research Scientist at the Hydro-Québec Research Institute (IREQ), Canada. He is also Associate Professor at the University of Quebec at Chicoutimi. He is actively involved in CIGRE B2-AG-06 Mechanical Aspects of Overhead Conductors and Fittings. He is part of the scientific committee of two NSERC Industrial Chairs. He developed transmission line accessories that are sold worldwide and for which he has two patents. He has been co-chairman of the 4th International Symposium on Cable Dynamics. He authored or co-authored more than 40 papers and two book chapters.
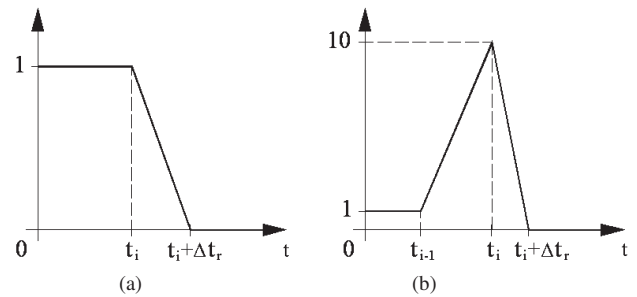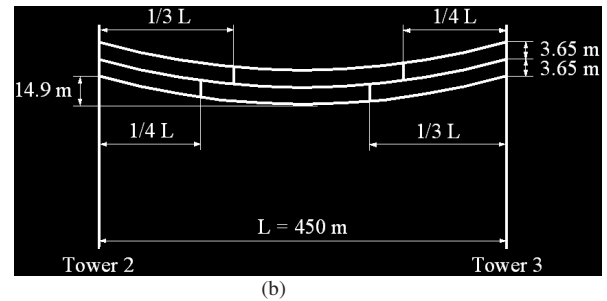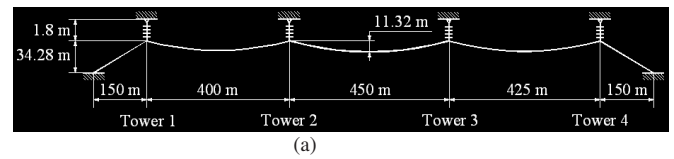
Fig. 1: Time functions for load removal

Fig. 2: Sketch of numerical models of unloaded test lines (not to scale), (a) configuration with single conductors, Test A, (b) middle span in configuration with vertical arrangement of three conductors, Test C (the top and bottom conductors are in the same vertical plane, but there is a transverse distance of 0.98 m between the vertical plane of the middle conductor and that of the other two conductors)
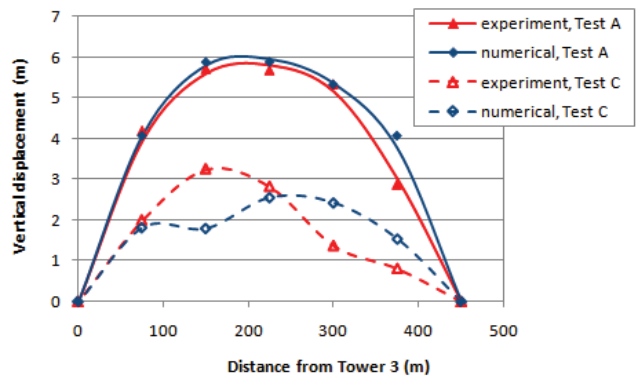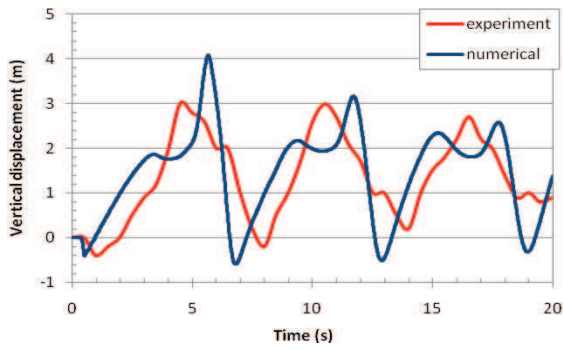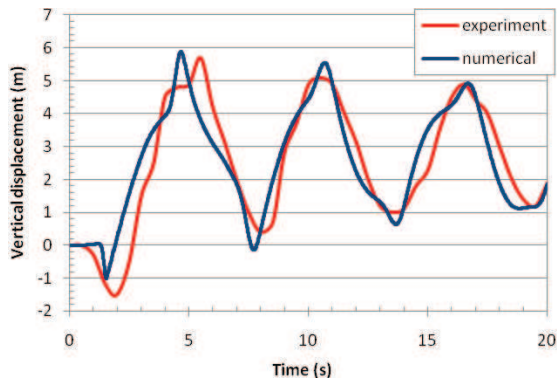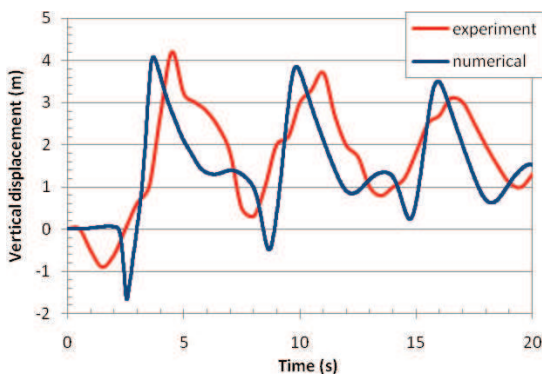

Fig. 3: Maximum vertical displacements of the conductor above the loaded position at different distances from Tower 3 for Tests A and C
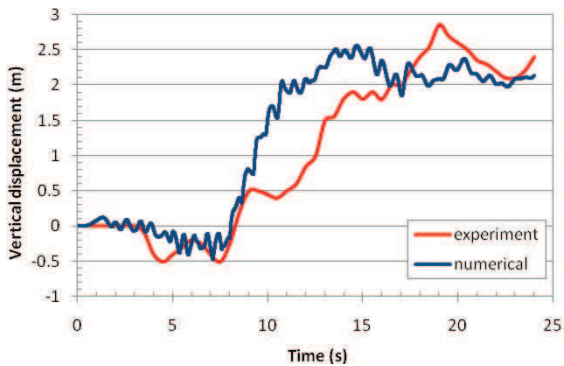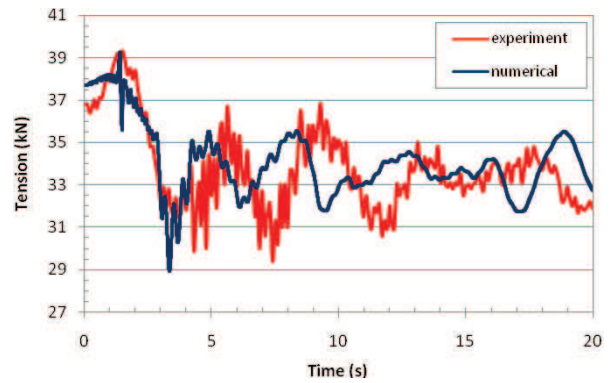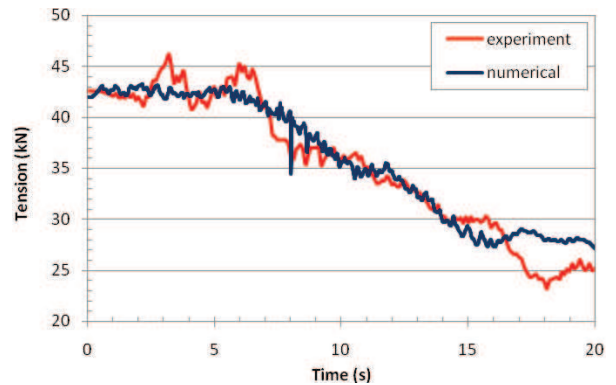
(a)

(b)

(c)

(d)

Fig. 4: Time histories of conductor vertical displacement during the vibration from the beginning of shedding propagation, (a) Test A, 375 m from Tower 3, (b) Test A, 225 m from Tower 3 (mid-span), (c) Test A, 75 m from Tower 3, (d) Test C, 225 m from Tower 3 (mid-span)
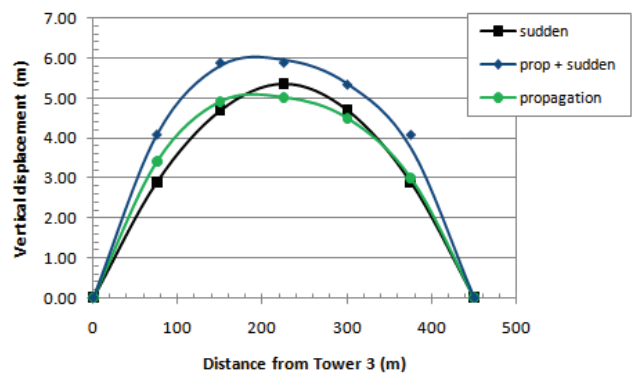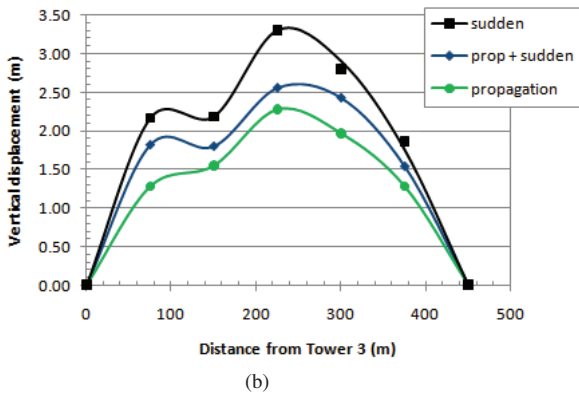

(a)

(b)

Fig. 5: Time histories of conductor tension at mid-span during the vibration from the beginning of shedding propagation, (a) Test A, (b) Test C

(a)

(b)

Fig. 6: Maximum vertical displacements of the conductor above the loaded position at different distances from Tower 3 for the three shedding processes: sudden shedding (sudden), propagating detachment followed by sudden fall (prop + sudden), and propagating shedding (propagation), (a) single conductor, (b) three conductors with interphase spacers
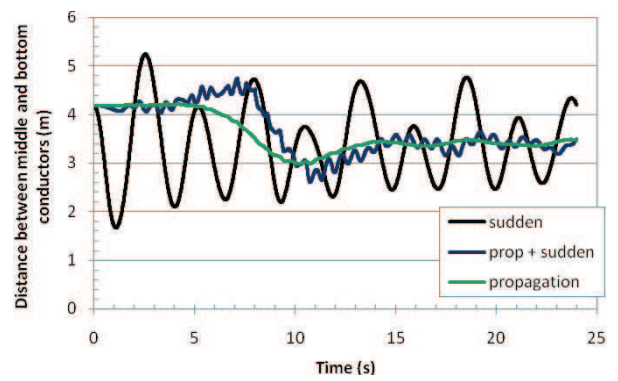

Fig. 8: Time histories of distance between the middle and bottom conductors at mid-span during the vibrations following the three shedding processes: sudden shedding (sudden), propagating detachment followed by sudden fall (prop + sudden), and propagating shedding (propagation)
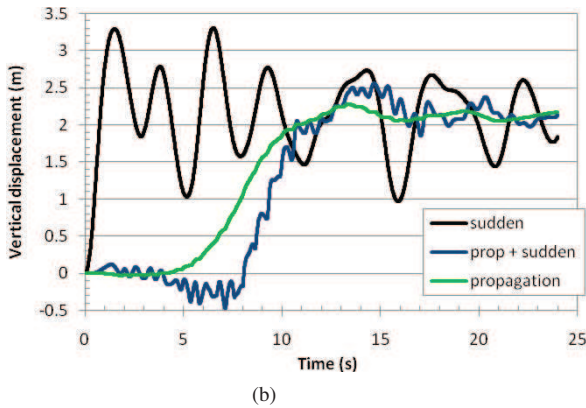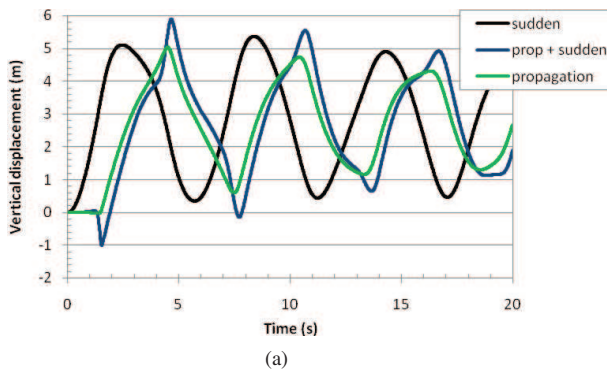

(a)

(b)

Fig. 7: Time histories of conductor vertical displacement at mid-span during the vibrations following the three shedding processes: sudden shedding (sudden), propagating detachment followed by sudden fall (prop + sudden), and propagating shedding (propagation), (a) single conductor, (b) three conductors with interphase spacers

TABLE I
SAG AND TENSION OF UNLOADED AND LOADED CONDUCTOR

Test	Unit	A	C
Initial sag	m	11.32	14.90
Additional sag – experiment	m	2.77	2.32
Additional sag – numerical	m	2.75	2.52
Initial tension	kN	33.4	25.4
Tension in loaded conductor – experiment	kN	36.6	42.6
Tension in loaded conductor – numerical	kN	37.7	41.9

TABLE II
MAXIMUM CONDUCTOR REBOUND AFTER SHEDDING, CONDUCTOR DROP BEFORE SHEDDING, AND PERIOD OF VIBRATION IN TEST A

	375 m		225 m		75 m	
	Exp.	Num.	Exp.	Num.	Exp.	Num.
Peak (m)	3.0	4.1	5.7	5.9	4.2	4.1
Drop (m)	-0.4	-0.4	-1.5	-1.0	-0.9	-1.7
Period (s)	6.2	6.1	5.6	6.0	6.1	6.1